



Recharge and spatial distribution of groundwater hydrochemistry in the Geum River basin, South Korea

Hanna Choi¹ · Chung-Mo Lee¹ · Dong Chan Koh¹ · Yoon Yeol Yoon¹

Received: 12 January 2021 / Accepted: 25 May 2021 / Published online: 21 June 2021
© Akadémiai Kiadó, Budapest, Hungary 2021

Abstract

Groundwater in the Geum River basin is a major agricultural and domestic water resource. In the present study, we collected 128 groundwater samples from four candidate regions (KS, KJ, NS, and BO) for hydrochemical analyses to identify large-scale groundwater distribution. Only 5.5% of samples showed natural background levels of NO₃-N and Cl, whereas about 65% of samples reflected the influence of external pollutants according to drinking water standards. Levels of tritium (³H) in groundwater in the BO region indicated rapid recharge over a uniform time span (2.88 ± 0.43 TU). The hydrochemical properties of water samples collected in this study suggest a sustainable water supply in the Geum River basin.

Keywords ³H · Cl · Geum river basin · Large-scale water supply · NO₃-N

Introduction

Global warming is characterized by the frequent occurrence of floods and droughts, which can have profound consequences for water resources [1, 2]. The quantity of groundwater remains constant despite climate change [3]; therefore, groundwater is important for mid- to long-range water resource planning for stable water supplement to cope with water scarcity [4, 5].

In 2018, groundwater in Korea was mainly utilized for domestic (1229 million m³/year; 42.5% of total usage) and agricultural (1485 million m³/year; 51.7%) applications [6]. Groundwater consumption in Korea is highest in Daejeon, Sejong, and Chungcheongnam-do, excluding Jeju Island [6]. Chungcheong-do, which encompasses Daejeon, Sejong, Chungcheongnam-do, and Chungcheongbuk-do, is located in the midwestern region of South Korea, facing the Yellow Sea. The Geum River is a major river in Korea that flows through Chungcheong-do; its estimated groundwater recharge rate reaches 3298 million m³/year, with about 91% (3012 million m³/year) occurring in the Chungcheong-do area [7]. Nevertheless, the accumulated summer

(June–August) precipitation in this area was 365 mm in 2019, which was less than in 2018 (588 mm), as well as the overall average for Korea (493 mm) [8]. Salt accumulation and nitrate contamination are increasing in this region due to the development of small and medium cities, agricultural activities, and livestock facilities. Seawater intrusion by excessive pumping of groundwater in coastal areas also contributes to the degradation of groundwater quality in midwestern South Korea [6, 7, 9].

In this study, we used contamination indicators including ionic and isotopic species to identify groundwater sources. These include nitrate nitrogen (NO₃-N) and chlorine (Cl) as anthropogenic inputs, fluoride (F⁻) as a geologic input, chloride (Cl⁻) and bromide (Br⁻) as seawater intrusion inputs. NO₃-N is present in natural water at very low concentrations, where concentrations > 3 mg/L are interpreted as having artificial origin [10, 11]. Potential sources of NO₃-N leaching include animal manure, domestic sewage, agricultural operations, and inflow from air pollution. The high solubility of this species facilitates inflow and migration into soil water and groundwater [12, 13]. High concentrations of NO₃-N (> 10 mg/L) in drinking water can cause methemoglobinemia, which leads to acute toxic responses to NO₂ exposure via oxygen transport [14]. Therefore, the NO₃-N drinking water standard for Korea has been established at 10 mg/L (~44 mg/L as NO₃) [15].

F⁻ is generally present in natural water at concentrations < 1 mg/L; it is usually derived from rock minerals such as

✉ Yoon Yeol Yoon
yyoon@kigam.re.kr

¹ Geologic Environment Division, Korea Institute of Geoscience and Mineral Resources, 124 Gwahang-ro, Yuseong-gu, Daejeon 34132, Korea

fluorite, apatite, amphiboles, and micas [10]. Low concentrations (<0.7 mg/L) of F^- in natural water can prevent tooth decay [16]. However, excessive F^- can cause dental fluorosis and bone weakness; therefore, F^- levels should be maintained within 1.5 mg/L [14].

Cl^- and Br^- concentrations can be influenced by seawater intrusion, domestic sewage, industrial waste water, de-icing salt dissolution, and bedrock mineral interactions. These ions represent stable species in the natural environment because they do not adsorb to other minerals or organic matter, or form non-soluble precipitations according to changes in the oxidation–reduction environment [17].

Tritium (3H ; $t_{1/2} = 12.43$ years, $E_{max} = 18.6$ keV) is a natural radioactive nuclide that is produced by cosmic ray bombardment of nitrogen and deuterium in the upper atmosphere. 3H enters the hydrological cycle in the form of tritiated water molecules (HTO), where it can be used as a conservative groundwater tracer as a component of the water molecule. When water infiltrates groundwater, it becomes isolated from the atmospheric 3H source and its 3H concentration decreases over time due to radioactive decay. Therefore, 3H is used as a groundwater dating tool for ages up to 100 years [18, 19].

Decreases in annual precipitation and active groundwater pumping can deplete water resources and lower its quality. For the sustainable use and efficient management of groundwater in midwestern South Korea, it is necessary to understand the recharge characteristics and spatial distribution of groundwater hydrochemistry. Therefore, we investigated the coastal and inland groundwater hydrochemistry of the Geum River basin regional water system. Specifically, we assessed the spatial distribution of groundwater hydrochemistry in the Chungcheong-do region, determined the type and sources of groundwater contaminants, and identified promising

candidate sites for large-scale groundwater supply to cope with potential water shortages.

Site description

The average annual temperature of South Korea for the past 30 years has been 10.9 °C, and the average annual precipitation is 1295 mm, indicating a temperate climate [8]. Our study site ($35^{\circ}58'33.71''$ – $37^{\circ}03'40.10''N$, $126^{\circ}07'13.25''$ – $128^{\circ}04'06.03''E$; Fig. 1) covers Sejong, Chungcheongnam-do, and Chungcheongbuk-do, but excludes Daejeon because it contains several industrial complexes, has a high population density, and therefore cannot meet our study objectives.

The area of the study site is approximately 12,294 km² and is bounded to the east by the southern Sobaek mountain range and to the west by the Yellow Sea. Thus, the topography of the site slopes downward from the east to the west, and agricultural fields and urban districts are mainly distributed in the west, whereas forests are distributed in the east. The geology of the study site is mainly composed of the Archean–Proterozoic Gyeonggi metamorphic complex, the Sobaegsan metamorphic complex, and Jurassic Daebo granitoids [20], in connection with the Mesozoic rift, as well as rocks from the Paleozoic Okcheon Supergroup (from Chungcheongbuk-do to Daejeon) and Great Limestone series (Chungcheongbuk-do). Large-scale plutonic rock has developed in the parallel Okcheon Belt, via the Jurassic Daebo orogeny. Because we examined groundwater over a large area in this study, we have simplified the bedrock geology to nine hydrogeological units: crystalline gneiss, intruded Cretaceous granite, intruded Jurassic granite, unconsolidated detrital deposits, metasedimentary rock (with preserved structure geometry), metasedimentary rock (depleted structure geometry), nonporous volcanic rocks, clastic sedimentary rocks, and carbonate rocks.

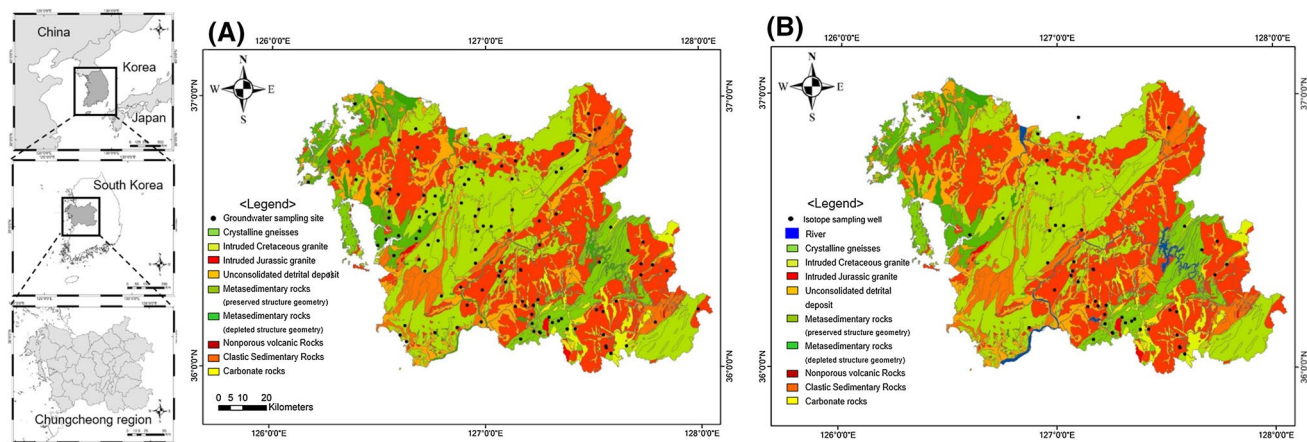


Fig. 1 Map of nine hydrogeological units and sampling points for **a** groundwater and **b** isotope analyses. Left panels show the geomorphological location of the study area

(with depleted structural geometry), nonporous volcanic rock, clastic sedimentary rock, and carbonate rock.

Materials and methods

Field sampling and ion analyses

Most of the groundwater sampling sites were located adjacent to rice paddies or dry farms during the agricultural off-season to avoid direct contamination and observe background hydrochemistry. We collected 128 groundwater samples for hydrochemical identification (Table 4) and analyzed 47 samples for isotope distribution in April 2020 (Table 1 and Fig. 8).

According to the field data, which included factors such as groundwater level and pumping rate, we selected four candidate sites to identify a promising site for a large-scale groundwater system: KS, KJ, NS, and BO. Hydrochemical, stable isotope ($\delta^{18}\text{O}$ and $\delta^2\text{H}$), and ^3H analyses were conducted to determine the groundwater recharge properties of these sites (Table 1).

In situ pH and electrical conductivity (EC) measurements were performed using a multi-parameter portable meter (WTW Multi 3620 IDS, Fisher Scientific, Sweden) and the uncertainty range of EC value was below ± 0.5 . Cation (Ca, K, Mg, and Na), anion (F, Cl, Br, NO_3 , and SO_4), stable isotope (^{18}O and ^2H), and radioisotope (^3H) analyses were performed in the laboratory. Alkalinity titration was performed to measure HCO_3 ion levels using 0.02 N hydrochloric acid and a Rondolino DL50 Titroprocessor (Mettler Toledo, Australia). All water samples were filtered through a 0.45 μm pore size cellulose acetate membrane (Advantec), stored in polypropylene bottles, and kept in a refrigerator at 4 $^\circ\text{C}$ for later chemical analyses. Cation samples were acidified with concentrated nitric acid to $\text{pH} < 2$. Cation and anion concentrations were analyzed using inductively coupled plasma optical emission spectrometry (ICP–OES, OPTIMA 7300DV, PerkinElmer, USA) and ion chromatography (Dionex Aquion, Thermo Scientific, USA), respectively. The sample ion concentration charge balance error was within $\pm 10\%$.

Isotope analyses

Oxygen (^{18}O) and hydrogen (^2H) isotopes were analyzed using cavity ring-down spectroscopy (L2140-i for isotopic H_2O ; Picarro, USA) and the results were compared to those of standard mean ocean water (V-SMOW). The stable isotope data of ^{18}O and ^2H are reported with the δ in ‰ deviation relative to V-SMOW and the uncertainties of isotope ratios were generally below $\pm 0.1\%$ for $\delta^{18}\text{O}$ and $\pm 0.5\%$ for $\delta^2\text{H}$.

Two local meteoric water regression lines (LMWLs) were plotted to describe the isotopic data for different seasons: $\delta\text{D} = 7.93\delta^{18}\text{O} + 8.11$ for summer precipitation and $\delta\text{D} = 7.79\delta^{18}\text{O} + 18.39$ for spring, autumn, and winter precipitation [21]. The slope and intercept of the regression line for wet season precipitation were virtually identical to those of the empirical global meteoric water line (GMWL) [22]:

$$\delta\text{D} = 8 \delta^{18}\text{O} + 10.$$

For ^3H analyses, groundwater samples were filtered through a 0.45 μm nuclear pore filter and distilled to remove impurities, followed by electrolytic enrichment as previously described [23]. The enriched sample was distilled and a 10 mL water sample was mixed with a 10 mL cocktail (Ultima Gold LLT, PerkinElmer) consisting of a mixture of scintillator, solvent, and surfactant. Subsequent ^3H measurements were performed using a low-level liquid scintillation counter (Wallac Quantulus 1220, PerkinElmer).

Geographic information system (GIS) database

A map of East Asian administrative boundaries (National Spatial Data Infrastructure Portal; <http://data.nsd.gov.kr/dataset/20171206ds00003>) was used as the GIS base map, with rivers (K-water; <http://www.wamis.gov.kr:8081/WaterMap2013/watermap.aspx?paramTab=searchmap>), hydrogeological units, and electrical conductivity (EC) as layers. Open source data were obtained from ArcGIS Online. Hydrogeological units were classified according to geological age, lithofacies, topography, and porosity (Table 2) [24]. EC spatial distribution was analyzed using inverse distance weighting (IDW) using the IDW spatial analyst tool in the ArcGIS ver. 10.7 software. Interpolation was performed using a distance index of 2, influence radius of 12 wells per central well, and an output raster cell size of 30 m \times 30 m.

Results and discussion

Regional hydrochemistry distribution

Most of the groundwater samples in the Chungcheong-do region were distributed in fields 3, 5, and 6 of the Durov diagram (Fig. 2). The pristine groundwater in this region is characterized by the Ca- HCO_3 water type, and is most influenced by simple dissolution of geologic materials or mixed natural/anthropogenic inputs (Table 5) [25]. Annual groundwater usage in this area has been stable since 2010, at about 39 million m^3/year , but decreased significantly in 2018 to about 28 million m^3/year [26]. Based on these data, seawater intrusion decreased with the change in pumping, and fresh groundwater increased the depth of the coastal

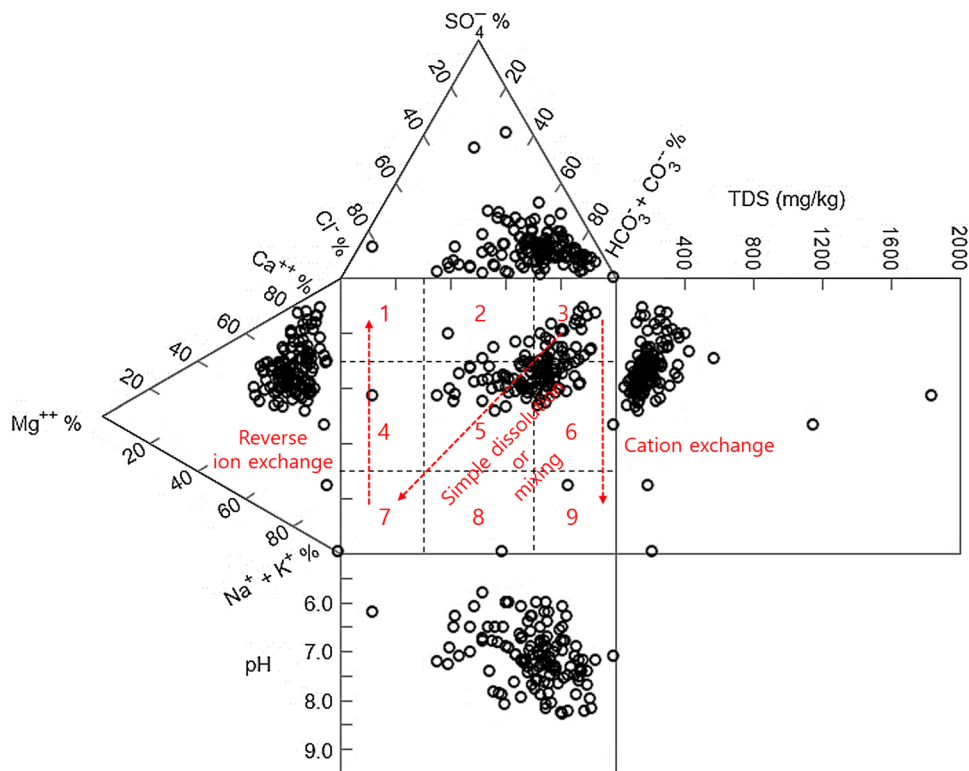
Table 1 Values of groundwater pH, depth, and electrical conductivity (EC) measured at the study sites and isotope values including $\delta^{18}\text{O}$, $\delta^2\text{H}$, deuterium excess, and tritium (^3H) concentrations of collected samples

Well ID	pH	Depth (m)	EC ($\mu\text{S}/\text{cm}$)	$\delta^{18}\text{O}$	$\delta^2\text{H}$ ‰ VSMOW	Deuterium excess	^3H TU
GW1	6.20	80	120	-7.74	-51.73	10.2	1.73 ± 0.14
GW2	7.40	71	150	-8.86	-58.77	12.1	1.59 ± 0.12
GW3	6.60	80	180	-8.03	-54.14	10.1	2.67 ± 0.14
GW4	6.80	80	220	-7.18	-49.56	7.90	1.78 ± 0.16
GW5	6.70	80	390	-7.72	-51.69	10.1	2.21 ± 0.26
GW6	7.10	80	264	-8.45	-56.65	10.9	2.24 ± 0.23
GW7	6.90	76	256	-8.31	-55.61	10.8	2.77 ± 0.28
GW8	6.50	82	222	-7.58	-51.60	9.00	2.03 ± 0.17
GW9	6.40	80	350	-7.38	-49.85	9.20	1.94 ± 0.19
GW10	7.40	80	150	-7.95	-56.52	7.05	1.75 ± 0.17
GW11	6.30	100	170	-8.07	-53.36	11.2	2.06 ± 0.21
GW12	6.80	80	430	-7.51	-51.04	9.07	1.24 ± 0.12
GW13	6.40	80	142	-7.13	-49.64	7.42	1.58 ± 0.09
GW14	7.90	100	380	-7.73	-51.97	9.87	< 0.3
GW15	7.50	108	320	-7.70	-51.46	10.2	1.93 ± 0.23
GW16	6.50	70	440	-8.05	-54.53	9.89	2.69 ± 0.17
GW17	6.50	60	350	-6.74	-48.49	5.47	9.10 ± 0.59
GW18	6.30	70	193	-8.45	-57.23	10.4	2.45 ± 0.22
GW19	7.20	70	254	-8.90	-60.38	10.8	1.96 ± 0.20
GW20	6.20	103	130	-8.21	-57.54	8.16	1.73 ± 0.12
GW21	7.40	100	285	-8.81	-58.84	11.7	2.72 ± 0.23
GW22	7.70	80	132	-8.81	-59.21	11.2	4.87 ± 0.56
GW23	7.00	100	165	-8.65	-57.90	11.3	1.60 ± 0.08
GW24	6.00	56	64	-9.19	-61.74	11.8	1.99 ± 0.15
GW25	7.10	80	134	-8.29	-57.11	9.20	2.88 ± 0.32
GW26	6.80	80	184	-8.08	-54.02	10.6	3.24 ± 0.28
GW27	5.80	100	175	-6.76	-46.96	7.10	2.99 ± 0.26
GW28	6.30	100	206	-8.56	-59.03	9.43	2.21 ± 0.18
GW29	6.50	50	130	-8.35	-54.82	11.9	2.64 ± 0.23
GW30	7.50	120	280	-7.57	-52.33	8.25	1.45 ± 0.09
GW31	6.00	80	115	-7.58	-51.84	8.78	2.91 ± 0.20
GW32	6.20	40	3390	-7.40	-48.33	10.9	2.03 ± 0.14
GW33	6.30	100	169	-8.62	-57.61	11.3	2.35 ± 0.16
GW34	7.10	150	131	-8.02	-54.26	9.91	0.90 ± 0.08
GW35	7.20	63	142	-8.04	-53.71	10.6	1.51 ± 0.13
GW36	7.63	86	291	-7.42	-55.20	4.17	3.26 ± 0.23
GW37	8.05	96	312	-7.09	-58.75	-2.00	3.32 ± 0.26
GW38	6.80	78	321	-7.42	-49.89	9.49	2.48 ± 0.23
GW39	6.75	80	179	-7.55	-49.30	11.1	3.00 ± 0.18
GW40	7.09	96	257	-8.45	-56.47	11.2	2.18 ± 0.14
GW41	7.66	120	281	-8.24	-54.36	11.6	2.64 ± 0.29
GW42	7.58	80	276	-6.94	-47.29	8.27	2.64 ± 0.22
GW43	7.36	95	205	-7.68	-52.83	8.60	2.09 ± 0.22
GW44	7.21	80	209	-8.51	-57.88	10.2	2.77 ± 0.18
GW45	8.16	100	210	-8.30	-54.92	11.5	1.01 ± 0.12
GW46	8.24	100	219	-9.24	-61.66	12.2	1.03 ± 0.07
GW47	7.54	31	394	-8.95	-59.35	12.3	2.20 ± 0.20

Table 2 Classification of hydrogeological units (modified from K-water, 2015 [24])

Units	Geological Age	Lithofacies	Topography	Porosity
Crystalline gneisses	Precambrian	Schist and gneiss	Mountain and hilly	Fracture
Intruded Cretaceous granite	Cretaceous, Paleogene, Neogene	Acidic intrusive igneous rock	Mountain and hilly	fracture
Intruded Jurassic granite	Jurassic	Acidic intrusive igneous rock	Mountain and hilly	fracture
Unconsolidated detrital deposit	Quaternary	Clay, silt, sand, and gravel	Plain and shore	primary opening
Metasedimentary rocks (preserved structure geometry)	Precambrian, age unknown	Low metamorphic sedimentary rock (slate, phyllite, quartzite, and fine-grained schist)	Mountain	fracture
Metasedimentary rocks (depleted structure geometry)	Precambrian, age unknown	Low metamorphic sedimentary rock (slate, phyllite, quartzite, and fine-grained schist)	Mountain	fracture
Nonporous volcanic rocks	Neogene, Cretaceous	Rhyolite, andesite, basic volcanic rock, and tuff	Mountain	Fracture
Clastic sedimentary rocks	Mesozoic, Permian	Clastic sedimentary rock (nonmarine and marine sediment rock)	Mountain	fracture
Carbonate rocks	Precambrian, Cambrian, Ordovician	Marine carbonate rock	Mountain and karst	fracture, corrosion cavities

Fig. 2 Durov diagram of hydrochemical facies of groundwater samples collected in the study area and major interaction processes (red arrows)



aquifer causing reverse cation exchange. However, the amount of total dissolved solids (TDS) was highest in this region among all groundwater samples (Fig. 2); therefore,

this site continues to experience seawater intrusion or effects from other pollutants.

Groundwater samples from fields 8 and 9 (G14 and G65 of Table 4, respectively) were collected from wells that were 100 and 210 m deep, respectively. These samples had lower Na^+ concentrations than the other samples, but the highest $\text{Na}^+ + \text{K}^+$ contribution, according to the major ion ratio data shown in Fig. 3A. The high concentrations of F^- indicated alkaline, Na-HCO_3 type water, developed through the dissolution of biotite from Mesozoic granitoids and Precambrian granitic gneiss [27].

The six sampling sites with the highest EC values ($> 625 \mu\text{S/cm}$) are shown in Fig. 3B; half of these sites are distributed inland, and half in coastal areas. These EC values were affected by seawater intrusion as well as input from other pollutants. Site A (G32 of Table 4) is bounded by the sea on three sides, and is about 200 m from a livestock facility; the groundwater sample from this site had the highest EC value ($3390 \mu\text{S/cm}$), likely due to input by seawater and livestock manure. Site D (G82 of Table 4), which had the highest population density ($1,057 \text{ people/km}^2$) and an urban area ratio of 42% [28, 29] had the second highest EC value. Sites B and C (G74 and G60 of Table 4, respectively) are located in coastal areas with dense facilities (65 million in 2010) and very high groundwater usage ($44 \text{ million m}^3/\text{year}$ in 2010) due to water supply shortages, with a 69.6% penetration rate in 2014 [28]. About 91% of all area in Sites E and F is non-urban (G88 and G65 of Table 4, respectively), with low population density (22 people/km^2) [28]; however, these sites had high groundwater EC and high F^- concentrations. The pristine groundwater at these sites likely reflects geologic characteristics.

Site-specific hydrochemistry

Bubble plots of each sampling site showing specific hydrochemical indicators are shown in Fig. 4. Most groundwater in the study area showed F^- concentrations $< 1.5 \text{ mg/L}$, which is the drinking water standard [15], except at two sites (Fig. 4a). The groundwater samples with the highest (6.86 mg/L , G65 plotted on the field 9) and second highest (3.36 mg/L , G92 plotted on the field 8) F^- concentration also had high Na-HCO_3 concentrations. The geology of these areas mainly comprises metasedimentary rocks from the Paleozoic Okcheon supergroup and Granitoid intrusions of Mesozoic age [20]. In these regions, F^- was likely released through the reaction of groundwater with rock-forming minerals in granite, which promoted calcite precipitation and fluorite dissolution at high pH [30, 31].

Cl^- concentrations varied greatly along the coast, and were highest at an inland sampling site with dense residential population and industrial facilities (Fig. 4b). The average background concentration of Cl^- in groundwater of South Korea is about $5\text{--}10 \text{ mg/L}$ [32, 33]; about 27.3% of our samples (35 sites) were within the background range. About 7%

of samples (nine sites) exceeded 50 mg/L Cl^- , reflecting water pollutants from urban areas [34], and one site (G32 of Table 4) exceeded the World Health Organization (WHO) drinking water standard of 250 mg/L , at which a salty taste is detected [14]. $\text{NO}_3\text{-N}$ concentrations exceeded 3 mg/L at about 65% of sites (83 sites) (Fig. 4C) and exceeded the drinking water standard at about 16% of sites (20 sites), presumably under the influence of anthropogenic sources such as livestock facilities, which are found within a 500 m radius of 55.5% of all groundwater sampling sites, and residential and industrial facilities (23.4%). The detailed values are presented on the Table 4.

Source estimation using ion indicators

A number of our samples were identified as endmembers, including those indicated in the lower left and upper right of Fig. 5a, which have a background concentration of Cl^- [32, 33, 35] and the highest natural (seawater intrusion) and anthropogenic (domestic/industrial sewage, animal manure) contamination among our samples. Cl^- concentration and EC were positively correlated ($R^2 = 0.7932$) among the groundwater samples; thus, this pair of samples are thought to have been similarly affected by contamination.

Groundwater contamination factors can be identified using the relationship between Cl/Br and Cl in the range above background concentration (10 mg/L Cl^-). Br^- is introduced into groundwater aquifers as a by-product of industrial activity or decomposition of organic matter in the soil layer [36]. Samples from agricultural areas with Cl^- concentrations $> 100 \text{ mg/L}$ (Fig. 5b) can be interpreted as pristine groundwater mixing with halite, sewage, animal waste (manure), basin brine, and landfill leachate [35]. Samples with Cl^- concentrations $> 10 \text{ mg/L}$ and with Cl/Br molar ratios greater than that of seawater (655 ± 4) indicate seawater intrusion of a coastal area.

The correlation between Cl^- and $\text{NO}_3\text{-N}$ concentrations (Fig. 5c) can be used to distinguish contamination sources for a range of pristine groundwater and that contaminated by synthetic fertilizer, road de-icer, manure, septic sources, and other mixed sources [37]. The thresholds of NO_3^- contamination for South Korea are 3.0 mg/L ($0.68 \text{ mg/L NO}_3\text{-N}$) for bedrock groundwater and 5.5 mg/L ($1.24 \text{ mg/L NO}_3\text{-N}$) for alluvial groundwater [38]. The background concentration of Cl^- in shallow gravel aquifers is typically $10\text{--}20 \text{ mg/L}$ in the USA and other countries [39]. About 14% of samples (18 sites) showed a background level of NO_3^- ($< 5.5 \text{ mg/L}$), and only about 5.5% (seven sites) showed background levels of both NO_3^- and Cl^- ($< 10 \text{ mg/L}$), which indicates that most Geum River basin groundwater samples were affected by natural or anthropogenic pollutants.

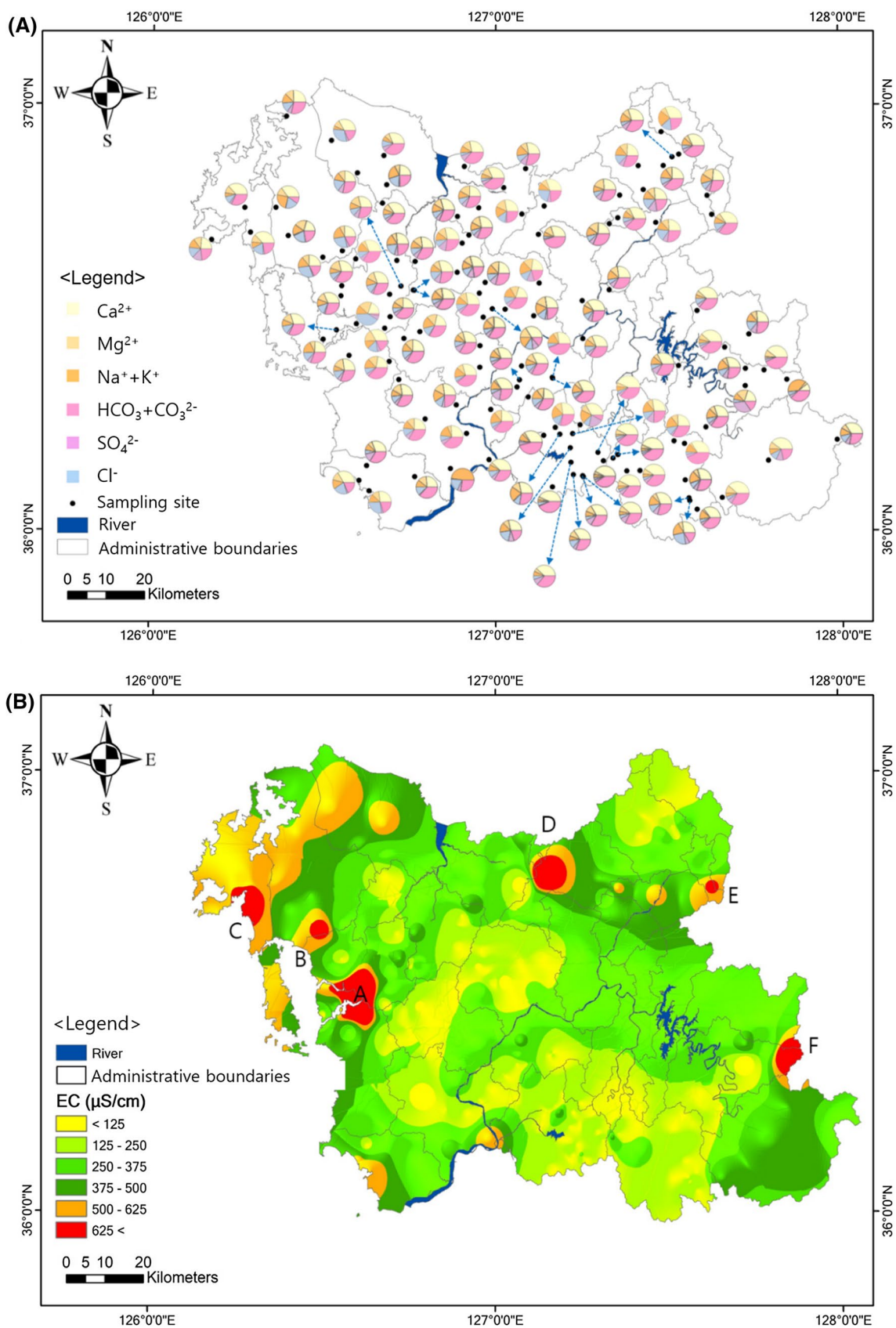


Fig. 3 Spatial distribution of (A) major ion species and electrical conductivity (EC) in the study area

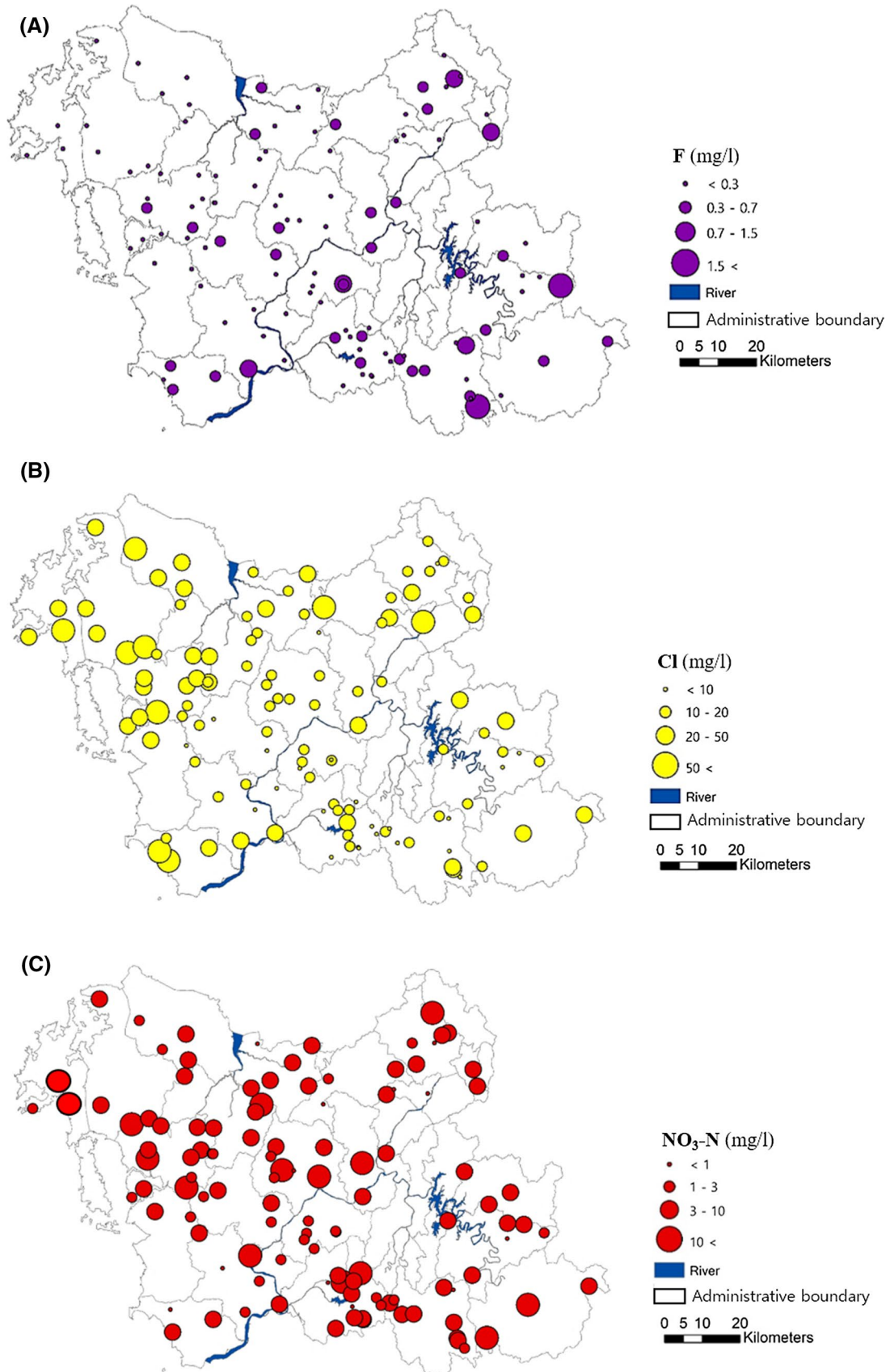


Fig. 4 Spatial distribution of natural and anthropogenic water components determined using **a** fluoride (F^-), **b** chloride (Cl^-), and **c** nitrate nitrogen (NO_3-N) as indicators

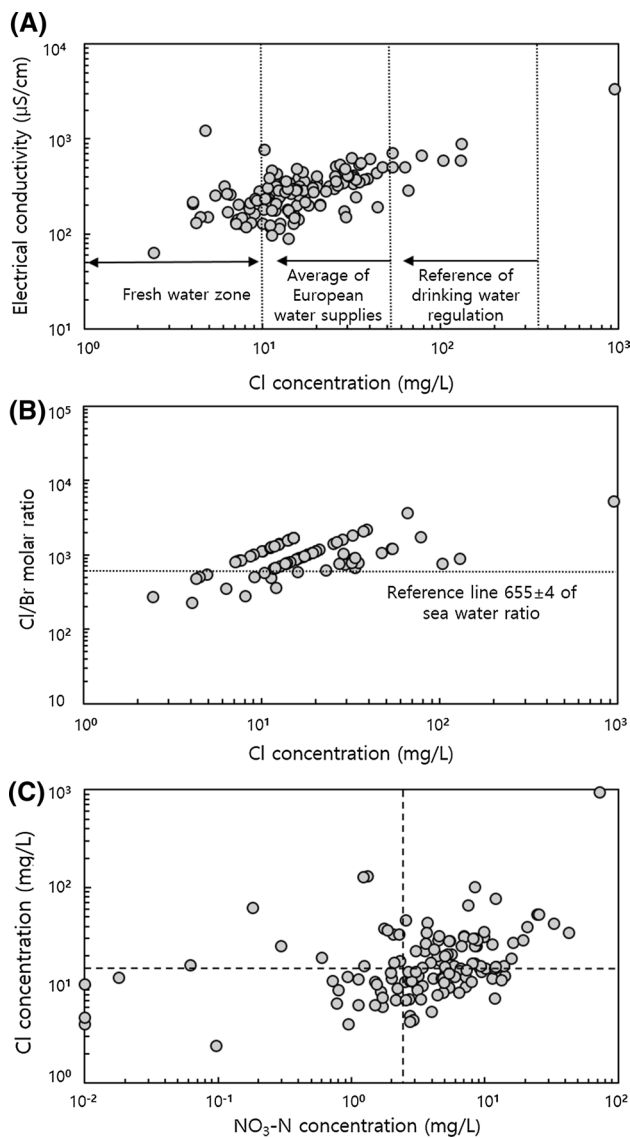


Fig. 5 Relationships between **a** Cl^- concentration and EC, **b** Cl^- concentration and Cl/Br molar ratio, and **c** NO_3-N and Cl^- . Axes are presented on a logarithmic scale

Regional isotope distribution

Oxygen–hydrogen isotope pairs ($\delta^{18}O$ – δ^2H) in samples collected in the study area were correlated with altitude and latitude, and a stronger positive correlation with altitude was detected (Fig. 6a, red arrow). Samples from higher-altitude regions showed depleted isotopic composition, apparently affected by winter precipitation, based on the winter LMWL. Samples from lower-altitude regions showed enriched isotopic composition and were affected mainly by precipitation recharge in summer. Some groundwater appears to have undergone evaporation (Fig. 6a, black arrow); these samples showed no significant relationship with contamination by F , Cl , or NO_3-N . The sample obtained closest to the coast (i.e., lowest altitude) showed the highest level of contamination in the study area and the greatest depletion of $\delta^{18}O$ – δ^2H , likely due to mixing with domestic sewage and livestock manure.

The Cl^- concentration of fresh groundwater was at the background level, at about 0.28 mEq/L (~ 10 mg/L Cl^-) [32, 33]; thus, about 27.3% of samples (35 sites) had background Cl^- levels. As the groundwater Cl^- concentration increased in this area, $\delta^{18}O$ enrichment was observed (Fig. 6b), likely due to the influence of evapotranspiration during recharge [40]. Mixing due to agricultural activity, domestic sewage, and livestock manure can increase Cl^- and NO_3-N concentrations and affect $\delta^{18}O$ enrichment [41]. The highest Cl^- concentration (26.5 mEq/L, G32 of Table 4) was associated with depleted $\delta^{18}O$, likely due to proximity to a livestock facility rather than seawater intrusion.

The distribution of 3H concentrations in Geum River basin groundwater is shown in Table 3. Similar 3H residence times were observed among regions, with averages of 2.19 ± 0.59 TU (1.03–2.88 TU) at KS, 2.15 ± 0.55 TU (0.90–2.91 TU) at KJ, 2.38 ± 1.08 TU (1.01–4.87 TU) at NS, and 2.48 ± 0.69 TU (1.14–3.60 TU) at BO. The 3H concentration distribution was narrow at KJ but broad at NS; values were higher at BO than in other regions (Fig. 7). Therefore, BO groundwater appears to be younger, with faster recharge times than observed in other regions [42, 43]. Values of 3H concentration < 0.5 TU indicate recharge prior to the 1950s,

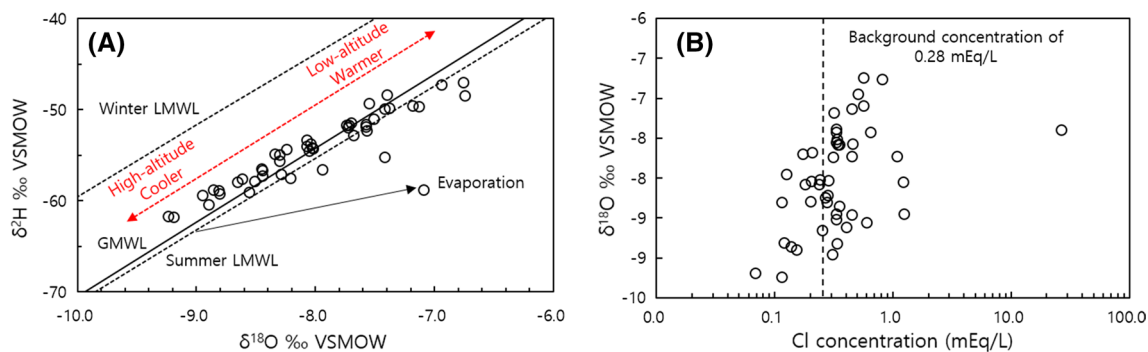


Fig. 6 a Stable oxygen–hydrogen isotope composition of groundwater samples collected in the study area. LMWL, local meteoric water line [21]; GMWL, global meteoric water line [22]. **b** Relationship

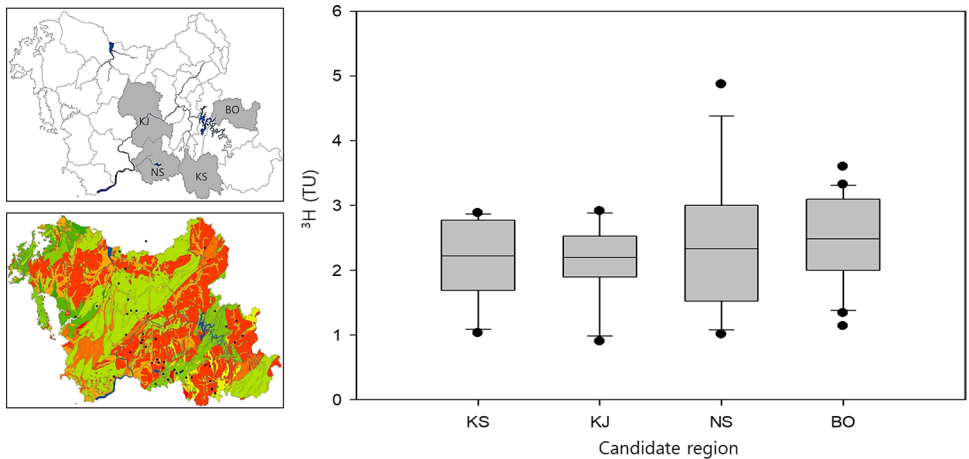
between Cl⁻ concentration and isotopic distribution of groundwater samples; reference line indicates the background Cl⁻ concentration for Korea, according to Cho et al. [32] and Park et al. [33]

Table 3 Tritium (³H) concentration of four candidate regions for large-scale groundwater supply: KS, KJ, NS, and BO

Region (samples)	Average ± standard deviation (TU)	Range (TU)
KS (13)	2.19 ± 0.59	1.03–2.88
KJ (12)	2.15 ± 0.55	0.90–2.91
NS (13)	2.38 ± 1.08	1.01–4.87
BO (22)	2.48 ± 0.69	1.14–3.60

indicating older groundwater, whereas those > 2 TU indicate younger groundwater. Most ³H values from the four candidate sites examined in this study are located between 1.5 to 3 TU, indicating recent recharge or slight mixing with old groundwater at these sites.

Fig. 7 Tritium (³H) concentrations in the four candidate regions for a large-scale groundwater supply system. Left panel shows the target area (upper) and sampling sites (lower) used for ³H analyses



Conclusion

We investigated regional groundwater hydrochemistry and isotopic distribution in 128 groundwater samples collected in Chungcheong-do (excluding Daejeon), which is highly dependent on groundwater for domestic and agricultural usage. Most of the sampling sites are located on rice paddies or dry farms, but are within a 500 m radius of livestock, residential, or industrial facilities. In the study area, groundwater is mainly recharged through precipitation and water is mainly of the Ca-HCO₃ type due to simple dissolution and/or mixing processes.

About 65% (83 sites) of all samples showed NO₃-N concentrations > 3 mg/L, indicating that the sampling aquifer was influenced by anthropogenic inputs, and about 16% (20 sites) exceeded the NO₃-N drinking water standard of Korea. Cl⁻ concentrations > 100 mg/L were observed at six sites in inland or coastal areas; these clearly indicated contaminant

mixing. High F⁻ concentrations were correlated with high Na⁺ and HCO₃⁻ concentrations due to interactions between the water and bedrock containing fluorine minerals.

Based on indicators of natural and anthropogenic contamination, the BO region is a promising candidate site for a large-scale groundwater system. The groundwater in this region has a relatively fast recharge time within a uniform time span, and contamination indicators were observed within background levels. Further groundwater sampling should be conducted at the BO site using a denser sampling strategy and more diverse indicators for the creation of a systematic preservation plan for long-term groundwater availability.

Appendix

See Tables 4 and 5, Fig. 8.

Table 4 Values of groundwater pH measured at the study sites and concentrations of major ion species (Ca, Mg, Na, K, HCO₃, Cl, and SO₄) and minor ion species (F, Br, and NO₃), and total dissolved solids (TDS) of collected 128 samples. All species expressed as mg/L unit except pH

ID	pH	Ca	Mg	Na	K	HCO ₃	F	Cl	Br	NO ₃	SO ₄	TDS
G01	6.20	19.0	5.03	10.5	1.03	74.8	0.046	11.1	0.05	11.1	11.3	174
G02	7.40	39.9	3.07	4.14	1.14	109	0.161	4.89	0.02	12.1	7.55	193
G03	6.60	17.1	4.30	6.90	2.49	51.1	0.027	10.1	0.02	13.7	16.3	133
G04	6.80	26.4	3.30	11.8	0.77	91.9	0.359	11.2	0.05	12.1	4.95	195
G05	6.70	31.0	6.38	10.3	1.26	97.1	0.000	15.9	0.04	5.49	11.0	206
G06	7.10	63.7	7.77	7.37	2.35	176	0.392	11.7	0.00	23.1	21.2	327
G07	6.90	60.0	6.55	5.99	2.31	157	0.319	9.79	0.00	31.5	18.3	306
G08	6.50	47.7	4.29	8.74	1.88	139	0.436	12.0	0.04	0.08	27.0	260
G09	6.40	19.5	5.14	11.7	1.75	75.1	0.318	11.6	0.04	4.94	11.8	165
G10	7.40	28.7	2.30	4.08	1.26	74.2	0.035	4.46	0.02	12.8	6.44	145
G11	6.30	14.2	3.66	9.70	1.34	62.4	0.000	6.38	0.00	4.98	5.23	132
G12	6.80	18.9	4.97	15.5	1.37	55.9	0.026	12.0	0.08	50.0	0.87	199
G13	6.40	19.0	4.41	13.8	1.24	60.8	0.065	15.8	0.06	25.9	4.59	185
G14	7.90	0.05	0.41	63.6	0.84	97.0	0.736	38.5	0.04	7.78	13.0	236
G15	7.50	17.2	3.22	9.15	1.00	68.1	0.112	6.12	0.00	7.49	2.80	139
G16	6.50	50.9	11.5	21.4	2.72	65.5	0.000	43.4	0.00	145	5.48	377
G17	6.50	28.7	11.6	14.1	2.29	110	0.052	20.0	0.04	22.0	16.5	255
G18	6.30	27.6	4.32	19.5	4.39	50.8	0.179	43.9	0.00	16.4	14.3	195
G19	7.20	61.5	8.59	2.82	1.36	206	0.157	5.38	0.00	17.5	11.8	327
G20	6.20	19.9	2.68	13.7	2.54	62.0	0.176	9.99	0.02	15.0	10.3	175
G21	7.40	68.4	8.42	8.54	5.93	213	0.424	11.8	0.00	18.1	17.3	365
G22	7.70	32.3	2.39	3.63	0.94	95.1	0.168	4.25	0.02	12.1	7.10	170
G23	7.00	29.0	5.47	13.9	2.45	99.2	0.747	8.94	0.02	13.8	18.0	201
G24	6.00	5.65	2.96	3.02	0.49	13.6	0.108	2.43	0.02	0.43	21.7	65.0
G25	7.10	27.1	1.50	12.5	1.13	89.8	1.871	7.09	0.00	9.49	7.25	176
G26	6.80	38.7	5.38	5.61	2.32	101	0.154	8.41	0.00	28.0	21.8	219
G27	5.80	24.8	5.00	13.7	2.21	53.8	0.042	28.7	0.06	24.3	17.8	192
G28	6.30	34.8	4.29	15.7	5.85	98.5	0.421	21.1	0.00	24.7	20.4	246
G29	6.50	21.0	6.50	9.46	3.38	26.1	0.022	12.5	0.02	62.0	14.5	171
G30	7.50	54.8	14.9	19.6	3.66	219	0.553	16.1	0.04	0.27	36.8	413
G31	6.00	13.9	5.14	11.4	1.59	73.1	0.026	12.4	0.02	4.11	9.07	160
G32	6.20	258	144	183	11.2	104	0.000	939	0.40	319	197	2193
G33	7.90	48.6	11.4	11.4	1.18	190	0.272	12.6	0.04	14.0	19.6	339
G34	6.10	15.5	2.54	9.01	1.49	11.4	0.000	7.48	0.02	52.6	22.9	143
G35	7.30	19.5	4.81	8.06	1.57	78.4	0.127	11.1	0.02	6.59	7.47	159
G36	6.00	16.0	5.75	13.0	4.46	44.7	0.131	15.0	0.02	40.3	17.3	174
G37	6.30	19.6	6.45	10.2	4.98	71.3	0.232	14.3	0.02	30.1	19.1	191
G38	7.20	35.0	6.96	29.2	1.93	136	0.000	33.4	0.11	9.03	20.0	285
G39	7.10	27.5	1.44	12.2	1.10	67.0	0.000	8.58	0.02	7.32	29.6	174
G40	7.20	34.7	2.12	2.56	1.03	105	0.139	7.25	0.02	14.5	2.66	182
G41	7.00	28.3	4.93	5.61	1.57	75.9	0.100	18.0	0.04	20.6	9.70	181
G42	7.40	19.2	6.07	7.19	0.79	32.0	0.000	15.4	0.04	53.7	6.42	159
G43	7.60	46.5	11.3	17.7	1.07	146	0.294	32.3	0.04	30.9	10.6	333
G44	6.50	36.2	6.28	31.0	3.09	76.9	0.221	65.8	0.04	33.0	11.8	293
G45	6.00	14.0	3.63	6.17	2.57	56.4	0.198	11.3	0.02	3.20	8.58	114
G46	7.30	34.0	12.3	10.6	1.31	124	0.255	20.9	0.04	23.2	10.3	268
G47	6.80	23.2	4.00	16.3	0.86	63.1	0.088	29.2	0.09	19.8	11.1	204
G48	6.10	17.3	5.74	10.6	1.03	47.7	0.185	14.0	0.02	41.5	3.26	174
G49	6.10	37.6	5.80	10.2	1.37	120	0.095	13.8	0.04	22.6	11.2	255
G50	6.00	19.8	5.00	8.77	4.16	47.0	0.126	14.9	0.02	29.0	17.1	161
G51	7.96	34.1	9.86	18.0	3.88	118	0.084	32.4	0.08	19.9	19.5	287

Table 4 (continued)

ID	pH	Ca	Mg	Na	K	HCO ₃	F	Cl	Br	NO ₃	SO ₄	TDS
G52	7.63	24.9	5.52	12.7	2.93	76.6	0.116	22.7	0.00	15.6	22.1	197
G53	8.05	46.7	4.46	6.76	1.61	134	0.048	20.0	0.04	19.5	14.2	258
G54	8.28	71.5	8.80	24.1	1.24	254	0.160	25.6	0.00	1.31	37.0	444
G55	8.10	53.0	12.9	27.8	2.57	171	0.177	62.5	0.00	0.80	35.1	390
G56	7.68	21.7	8.53	13.1	1.19	90.1	0.000	14.0	0.00	28.8	12.3	215
G57	7.86	43.2	4.97	17.4	1.13	134	0.357	17.1	0.00	17.4	30.8	295
G58	7.43	25.3	3.72	18.0	0.72	74.0	0.000	16.7	0.00	37.2	16.0	232
G59	7.86	42.0	11.9	25.8	2.01	123	0.000	46.8	0.10	11.3	59.8	348
G60	7.84	62.8	11.9	15.0	3.04	116	0.000	53.4	0.10	108	8.93	397
G61	7.88	77.4	13.9	12.7	0.95	202	0.000	40.0	0.00	91.4	17.5	479
G62	6.80	29.3	3.87	11.6	0.61	115	0.000	11.8	0.04	8.88	12.1	221
G63	6.75	16.6	3.06	9.93	1.96	47.1	0.305	11.8	0.02	20.9	15.7	145
G64	7.09	19.5	6.82	13.3	0.83	50.8	0.000	15.8	0.00	61.0	6.04	202
G65	8.23	10.8	1.70	41.3	0.74	109	6.865	10.3	0.00	6.79	9.85	215
G66	7.66	32.3	6.24	7.44	2.16	98.1	0.000	9.52	0.00	23.8	21.3	212
G67	7.23	38.0	7.67	29.2	2.53	32.2	0.000	34.8	0.10	189	1.60	365
G68	7.58	20.9	5.96	15.0	1.09	88.2	0.000	18.0	0.04	10.1	12.3	213
G69	7.36	19.1	2.67	12.6	0.50	92.9	0.914	7.28	0.00	11.9	2.24	185
G70	6.75	17.9	9.68	14.3	1.50	58.1	0.000	31.8	0.09	43.8	1.88	196
G71	7.50	48.4	6.51	11.0	1.59	182	0.000	27.1	0.00	15.8	23.4	339
G72	7.42	25.3	4.37	14.7	0.53	91.2	0.318	12.4	0.00	26.4	8.86	220
G73	7.21	15.5	3.54	11.9	0.41	61.3	0.163	11.8	0.00	21.6	4.04	169
G74	6.93	40.2	9.89	27.4	1.54	85.7	0.000	77.9	0.10	52.8	7.14	347
G75	8.16	29.6	2.15	9.95	0.84	122	0.615	4.05	0.04	0.04	9.17	200
G76	7.26	37.6	5.95	14.5	0.85	127	0.450	23.5	0.00	18.3	15.7	268
G77	7.40	30.1	4.09	13.2	0.76	71.9	0.380	14.8	0.00	44.8	13.2	220
G78	7.02	28.5	7.37	15.7	1.47	104	0.301	12.3	0.00	31.5	19.0	251
G79	6.91	31.6	7.26	16.4	1.32	72.0	0.066	27.3	0.08	71.8	2.27	270
G80	7.69	40.0	8.33	23.7	2.99	127	0.000	25.3	0.00	38.4	31.9	330
G81	7.97	30.9	7.12	7.43	1.34	138	0.061	6.55	0.00	3.43	5.55	222
G82	6.80	102	17.0	38.6	1.93	240	0.309	130	0.00	5.79	42.5	614
G83	8.10	29.5	11.5	9.31	4.53	105	0.055	16.0	0.00	40.7	20.3	261
G84	7.37	21.8	6.02	7.23	2.13	74.7	0.137	8.45	0.00	21.4	14.1	176
G85	8.26	31.7	4.52	15.0	1.49	108	0.202	6.30	0.04	6.65	33.8	219
G86	7.65	17.7	4.83	8.71	0.83	68.6	0.155	11.2	0.00	12.4	11.5	162
G87	7.20	27.8	4.07	18.2	1.32	128	0.751	9.02	0.04	3.52	8.57	222
G88	8.18	57.1	7.00	16.2	1.92	175	0.717	31.5	0.00	30.9	14.7	359
G89	7.57	23.6	10.5	15.4	0.81	88.3	0.176	16.9	0.04	35.7	15.8	242
G90	7.78	31.5	8.58	12.0	1.59	90.7	0.331	15.5	0.04	22.1	29.8	241
G91	7.60	27.6	3.85	11.1	0.48	123	0.497	9.28	0.00	9.69	5.43	219
G92	7.10	112	10.8	147	2.25	865	3.364	4.76	0.00	0.00	0.00	1196
G93	7.13	24.8	7.62	11.8	0.99	83.0	0.000	11.3	0.00	59.0	14.6	238
G94	6.85	29.0	8.33	13.9	0.68	108	0.000	20.1	0.00	22.2	16.3	247
G95	7.27	82.4	15.1	12.9	1.60	140	0.000	130	0.33	5.42	17.3	417
G96	6.52	18.7	3.74	18.6	1.85	56.1	0.000	25.3	0.04	37.2	4.03	199
G97	6.52	29.1	7.21	13.6	2.93	98.6	0.000	36.9	0.04	8.21	20.6	225
G98	6.71	25.2	7.87	16.1	1.62	68.3	0.050	18.9	0.04	69.4	8.81	248
G99	7.18	75.8	5.48	20.0	0.88	208	0.000	35.6	0.00	43.6	24.0	450
G100	6.90	21.5	7.30	8.85	0.58	80.3	0.000	14.4	0.04	32.3	9.63	199
G101	6.58	15.0	1.83	10.8	0.72	66.9	0.077	7.62	0.02	7.58	8.43	143
G102	7.33	36.9	4.29	13.5	0.51	136	0.096	10.7	0.00	21.8	15.4	264

Table 4 (continued)

ID	pH	Ca	Mg	Na	K	HCO ₃	F	Cl	Br	NO ₃	SO ₄	TDS
G103	6.81	33.5	8.45	16.4	4.14	88.8	0.322	34.9	0.00	16.0	38.9	252
G104	7.34	27.8	5.99	17.3	1.04	123	0.000	19.2	0.04	2.66	12.8	243
G105	7.21	14.6	4.21	8.49	2.28	55.4	0.422	14.0	0.00	11.8	9.82	134
G106	7.13	29.5	3.48	10.2	1.04	96.0	0.404	10.3	0.04	0.04	28.4	209
G107	7.02	50.0	11.0	21.3	1.79	82.7	0.000	53.7	0.10	111	6.39	368
G108	6.79	27.7	8.60	12.3	1.35	117	0.457	22.7	0.08	13.4	4.34	244
G109	7.11	58.1	13.9	29.1	1.53	131	0.622	103	0.30	37.2	14.0	420
G110	6.94	18.5	2.66	13.8	1.04	41.3	0.027	15.1	0.02	52.2	0.86	182
G111	7.25	31.3	5.35	11.1	2.09	110	0.395	15.3	0.00	14.9	25.0	235
G112	7.01	8.08	3.34	7.27	0.45	36.6	0.389	8.05	0.07	19.4	1.53	107
G113	7.09	21.3	6.22	11.1	0.50	87.4	0.063	17.2	0.04	9.17	7.97	189
G114	8.24	22.1	1.29	9.23	0.29	84.8	0.871	4.06	0.00	4.21	7.39	157
G115	7.54	59.1	6.36	4.08	0.71	167	0.312	10.9	0.00	35.0	12.8	304
G116	7.34	22.0	5.76	10.4	0.89	71.0	0.442	13.3	0.00	23.9	11.6	182
G117	6.65	42.4	8.44	17.3	0.90	122	0.000	33.3	0.08	9.97	29.0	302
G118	6.91	24.5	2.81	12.0	0.83	82.7	0.058	13.8	0.04	13.3	10.1	187
G119	7.33	33.8	11.6	11.0	0.77	115	0.241	28.4	0.04	23.7	15.2	268
G120	7.08	39.6	10.9	13.9	1.54	129	0.000	30.2	0.00	37.9	9.88	301
G121	7.33	10.5	3.95	7.38	0.31	51.5	0.046	7.10	0.02	11.3	4.35	120
G122	7.25	33.1	8.14	12.0	0.79	94.2	0.349	26.3	0.04	50.2	4.62	257
G123	6.91	24.7	9.74	10.3	0.55	112	0.353	13.5	0.04	8.68	14.9	224
G124	6.90	42.9	14.2	15.8	1.10	133	0.000	29.0	0.00	38.6	27.3	334
G125	7.19	36.1	14.5	11.4	2.09	114	0.000	30.1	0.00	36.3	26.3	301
G126	7.55	64.8	11.4	8.63	2.15	171	0.000	15.5	0.00	52.9	27.6	371
G127	7.07	64.8	9.86	14.3	2.89	108	0.687	29.1	0.00	85.9	41.0	391
G128	7.18	42.0	5.75	14.8	1.81	104	0.338	25.6	0.00	29.5	20.9	271

*This table shows all groundwater samples, and the ID of samples different from sample labels in Table 1 to distinguish all sampling points from isotope sampling points

Table 5 Water type classifications for each field shown in Fig. 3, according to Lloyd and Heathcoat (1985) [25]

Field no	Water type
1	Ca–Cl dominant. Possibility of reverse ion exchange from Na-Cl type water
2	Ca-SO ₄ dominant. Recharge water in lava or gypsiferous deposit
3	Ca-HCO ₃ dominant. Recharge water in limestone, sandstone, and many aquifers
4	This water type presumed reverse ion exchange of Na-Cl type water
5	No dominant ion in this type water. Simple dissolution or mixing
6	This water type is presumed Mg related with the dolomite and Na related with the ion exchange
7	Na-Cl dominant and end-point water type
8	Na-SO ₄ dominant. Unusual water type and or dissolution influence
9	Na-HCO ₃ dominant and possibility of ion exchange water

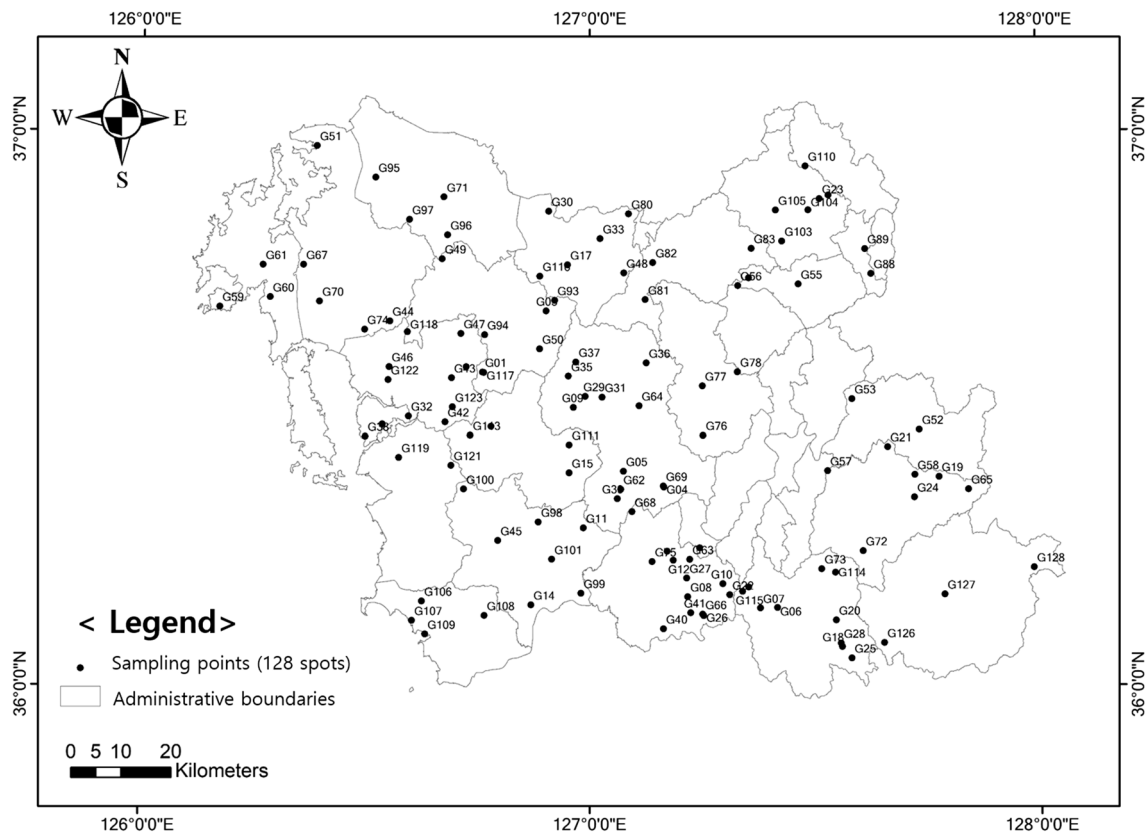


Fig. 8 A simplified sampling points map of Geum River basin, South Korea

Acknowledgements This work was supported by the Basic Research Project (21-3411) of the Korea Institute of Geoscience and Mineral Resources (KIGAM), funded by the Ministry of Science and Information and Communications Technology. We thank the other members of the Groundwater Research Center at KIGAM for their help with system setup and operation, data acquisition, and sample analyses. We also thank Dr. Min Han at the Geological Research Center at KIGAM for his considered advice regarding the geology of the study site.

References

- IPCC (Intergovernmental Panel on Climate Change) (2014) Jimenez, B.E., T. Oki, N.W. Arnell, G. Benito, J.G. Conley, P. Döll, T. Jiang, and S.S. Mwakalila. Freshwater resources. In: Climate Change 2014: Impacts, Adaptation and Vulnerability. Contribution of Working Group II to the Fifth Assessment Report of the Intergovernmental Panel on Climate Change. Field, C.B., V.R. Barros, D.J. Dokken, K.J. Mach, M.D. Mastrandrea, T.E. Bilir, M. Chatterjee, K.L. Ebi, Y.O. Estrada, R.C. Genova, B. Girma, E.S. Kissel, A.N. Levy, S. MacCracken, P.R. Mastrandrea, and L.L. White (eds.) Cambridge University Press, Cambridge, United Kingdom and New York, NY, USA.
- Payus C, Huey LA, Adnan F, Rimba AB, Mohan G, Chapagain SK, Gasparatos A, Roder G, Fukushi K (2020) Impact of extreme drought climate on water security in North Borneo: case study of Sabah. *Water* 12(4):1135
- Bates BC, Kundzewicz ZWW, Wu S, Palutikof JP (2008) Linking climate change and water resources: impacts and responses. IPCC Secretariat, Geneva
- Foster S, Ait-Kadi M (2012) Integrated water resources management (IWRM): how does groundwater fit in? *Hydrogeol J* 20(3):415–418
- van Geldern R, Baier A, Subert HL, Kowol S, Balk L, Barth JA (2014) Pleistocene paleo-groundwater as a pristine fresh water resource in southern Germany—evidence from stable and radiogenic isotopes. *Sci Total Environ* 496:107–115
- ME (Ministry of Environment) and K-water (2019) Groundwater annual report 2019. Sejong, Daejeon
- MOLIT (Ministry of Land, Infrastructure and Transport) (2017) National Groundwater Management Plan (2017–2026). Sejong
- KMA (Korea Meteorological Administration), Climate information in weather. https://www.weather.go.kr/weather/climate/past_cal.jsp. Accessed 15 Dec 2020
- Lee CM, Hamm SY, Cheong JY, Kim K, Yoon H, Kim M, Kim J (2020) Contribution of nitrate-nitrogen concentration in groundwater to stream water in an agricultural head watershed. *Environmental Research* 109313
- Hem JD (1985) Study and interpretation of the chemical characteristics of natural water (Vol. 2254). Department of the Interior, US Geological Survey, Reston
- Madison RJ, Brunett JO (1985) Overview of the occurrences of nitrate in groundwater of the United States. In: National Water Summary 1984: Hydrologic Events, Selected Water-Quality Trends, and Ground-Water Resources. United States Geological Survey Water Supply Paper 2275, p 93–105

12. Bouchard DC, Williams MK, Surampalli RY (1992) Nitrate contamination of groundwater: sources and potential health effects. *J Am Water Works Ass* 84(9):85–90
13. Wakida FT, Lerner DN (2005) Non-agricultural sources of groundwater nitrate: a review and case study. *Water Res* 39(1):3–16
14. WHO (World Health Organization) (2017) Guidelines for drinking-water quality. Fourth edition incorporating the first addendum. <http://apps.who.int/iris/bitstream/10665/254637/1/9789241549950-eng.pdf?ua=1>. Accessed 15 Dec 2020
15. ME (Ministry of Environment) (2020) Drinking Water Management Act. <https://law.go.kr/LSW/eng/LS/Sc.do?menuId=0&query=&subMenu=5#AJAX>. Accessed 15 Dec 2020
16. Gooch BF (2015) U.S. public health service recommendation for fluoride concentration in drinking water for the prevention of dental caries. *Public Health Reports* 130(4):318–331
17. Fetter CW (2018) Applied hydrogeology. Waveland Press, Long Grove
18. Clark ID, Fritz P (1999) Environmental isotopes in hydrology. Lewis Publishers, New York, pp 179–186
19. Kazemi GA, Lehr JH, Perrochet P (2006) Groundwater age. Wiley, New Jersey, pp 84–92
20. MOLIT (Ministry of land, infrastructure, and transport) and NGII (National geographic information institute) (2018) The National Atlas of Korea, Volume II: Natural environment and land. Jinhan M&B, Seoul, p 244
21. Lee KS, Lee CB (1999) Oxygen and hydrogen isotopic composition of precipitation and river waters in South Korea. *J Geol Soc Korea* 35:73–84 (in Korean with English abstract)
22. Craig H (1961) Isotopic variations in meteoric waters. *Science* 133:1702–1703
23. Yoon Y, Lee K, Ko K (2010) Development and validation of Ni-Ni electrolytic enrichment method for tritium determination in samples of underground waters of Jeju Island. *J Radioanal Nucl Chem* 286(2):591–595
24. K-water (2015) Basic groundwater survey, groundwater map production, and management guidelines. Ministry of Land, Infrastructure and Transport and K-water, Daejeon, p 163
25. Lloyd JW, Heathcote JAA (1985) Natural inorganic hydrochemistry in relation to ground water. Clarendon Press, Oxford
26. GIMS (National Groundwater Information Management and Service Center), Statistics in Groundwater in Korea. http://www.gims.go.kr/en/gims_start.do. Accessed 15 Dec 2020
27. Choi BY, Yun ST, Kim KH, Kim JW, Kim HM, Koh YK (2014) Hydrogeochemical interpretation of South Korean groundwater monitoring data using self-organizing maps. *J Geochem Explor* 137:73–84
28. KOSIS (Korean Statistical Information Service) (2019) Resident Registration Population. Daejeon
29. LH (Korea Land and Housing Corporation) (2019) The Present Status of Urban Planning. Jinju
30. Rao NR, Rao N, Rao KSP, Schuiling RD (1993) Fluorine distribution in waters of Nalgonda district, Andhra Pradesh, India. *Environ Geol* 21(1–2):84–89
31. Hwang J (2001) Fluorine distribution and attenuation of groundwater within limestone and granite from Keumsan–Wanju fluorite mineralized zone. *Econ Environ Geol* 34(1):105–117
32. Cho BW, Lee BD, Yoon W, Im HC (2003) Study on the possibility of seawater intrusion in the Ulsan area using Br: Cl weight ratios of groundwater. *Econ Environ Geol* 36(5):339–347
33. Park SC, Yun ST, Chae GT, Yoo IS, Shin KS, Heo CH, Lee SK (2005) Regional hydrochemical study on salinization of coastal aquifers, western coastal area of South Korea. *J Hydrol* 313:182–194
34. Yoon W, Ji SJ, So CS (2003) The hydrochemical and stable isotope characteristics of shallow groundwater near the Gwangju stream. *Econ Environ Geol* 36(6):441–455
35. Mullaney JR, Lorenz DL, Arntson AD (2009) Chloride in groundwater and surface water in areas underlain by the glacial aquifer system, northern United States (vol. 5086). US Geological Survey, Reston
36. Gerritse RG, George RJ (1988) The role of soil organic matter in the geochemical cycling of chloride and bromide. *J Hydrol* 101(1–4):83–95
37. Taylor SJ, Kelly WR, Panno SV, Weck R, Zheng W, Zhang Y, Liu WT (2014) Karst groundwater contaminants in western Illinois: comparison of current conditions with historical data. Illinois Natural History Survey, Prairie Research Institute, University of Illinois, Champaign, p 53
38. Kim KH, Yun ST, Kim HK, Kim JW (2015) Determination of natural backgrounds and thresholds of nitrate in South Korean groundwater using model-based statistical approaches. *J Geochem Explor* 148:196–205
39. Panno SV, Hackley KC, Hwang HH, Greenberg SE, Krapac IG, Landsberger S, O'Kelly DJ, (2006) Characterization and identification of Na-Cl sources in ground water. *Groundwater* 44(2):176–187
40. Han D, Currell MJ (2018) Delineating multiple salinization processes in a coastal plain aquifer, northern China: hydrochemical and isotopic evidence. *Hydrol Earth Syst Sci* 22:3473–3491
41. Re V, Sacchi E (2017) Tackling the salinity-pollution nexus in coastal aquifers from arid regions using nitrate and boron isotopes. *Environ Sci Pollut Res* 24(15):13247–13261
42. Koh DC, Chae GT (2008) Estimation of mixing properties and mean residence time using ^3H for groundwater in typical geothermal and CO_2 -rich areas in South Korea. *J Geol Soc Korea* 44(4):507–522
43. Jung YY, Koh DC, Yoon YY, Kwon HI, Heo J, Ha K, Yun ST (2019) Using stable isotopes and tritium to delineate groundwater flow systems and their relationship to streams in the Geum River basin, Korea. *J Hydrol* 573:267–280

Publisher's Note Springer Nature remains neutral with regard to jurisdictional claims in published maps and institutional affiliations.